Climate Change Drivers

Daniel Pangburn

Abstract: Thermalization and the complete dominance of water vapor in reverse-thermalization explain why atmospheric carbon dioxide (CO_2) has no significant effect on climate. Reported average global temperature (AGT) since before 1900 is accurately (98% match with measured trend) explained by a combination of ocean cycles, sunspot number anomaly time-integral and increased atmospheric water vapor.

I.   Introduction

The only way that energy can significantly leave earth is by thermal radiation. Only solid or liquid bodies and greenhouse gases(ghg) can absorb/emit in the wavelength range of terrestrial radiation. Non-ghg gases must transfer energy to ghg gases (or liquid or solid bodies) for this energy to be radiated.

The word 'trend' is used here for temperatures in two different contexts. To differentiate, α-trend is an approximation of the net of ocean surface temperature oscillations after averaging-out the year-to-year fluctuations in reported average global temperatures. The term β-trend applies to the slower average energy change of the planet which is associated with change to the average temperature of the bulk volume of the material (mostly ocean water) involved.

Some ocean cycles have been named according to the particular area of the oceans where they occur. Names such as PDO (Pacific Decadal Oscillation), ENSO (el Nino Southern Oscillation), and AMO (Atlantic Multi-decadal Oscillation) might be familiar. They report the temperature of the water near the surface. The average temperature of the bulk water that is participating in these oscillations cannot significantly change so quickly because of high thermal capacitance [1].

This high thermal capacitance absolutely prohibits the rapid (year-to-year) AGT fluctuations which have beenreported, frombeing a result of any credible forcing. According to one assessment [1], the time constant is about 5 years. A likely explanation for the reported year-to-year fluctuations is that theyare stochastic phenomena in the overall process that has been used to determine AGT. A simple calculation shows the standard deviation of the reported annual average measurements to be about ±0.09 K with respect to the trend. The temperature fluctuations of the bulk volume near the surface of the planet are more closely represented by the fluctuations in the trend. The trend is a better indicator of the change in global energy; which is the difference between energy received and energy radiated.

The kinetic theory of gases, some thermodynamics and the rudiments of quantum mechanics provide a rational explanation of what happens when ghg absorb photons of terrestrial thermal radiation.

Refutation of significant influence from CO_2

There is multiple evidence (most identified earlier [2]) that CO_2 has no significant effect on climate:
1. In the late Ordovician Period, the planet plunged into and warmed up from the Andean/Saharan ice age, all at about 10 times the current CO_2 level [3].
2. Over the Phanerozoic eon (last 542 million years) there is no correlation between CO_2 level and AGT [3, 4].
3. During the last and previous glaciations AGT trend changed directions before CO_2 trend [2].
4. Since AGT has been directly and accurately measured world wide (about 1895), AGT has exhibited up and down trends while CO_2 trend has been only up. [2]
5. Since about 2001, the measured atmospheric CO_2 trend has continued to rise while the AGT trend has been essentially flat. [21, 13]

Thermalization refutes CO_2 influence on climate. (rev 10/21/16)

The relaxation time (amount of time that passes between absorption and emission of a photon by a molecule) for CO_2 in the atmosphere is about 6μsec [5, 6]. The elapsed time between collisions between gaseous molecules at sea level average temperature and pressure is about 0.0002 μsec [7]. Thus, at sea level conditions, it is approximately 6/0.0002 = 30,000 times more likely that a CO_2 molecule, after it has absorbed a photon, will bump into another molecule, losing at least part of the momentum and energy it acquired from the photon. After

multiple collisions, essentially all of the added photonic energy becomes distributed among other molecules and the probability of the CO_2moleculeemitting a photon at sea level conditions becomes negligible. The process of distribution of the energy to other molecules is thermal conduction in the gas. The process of absorbing photons and conducting the absorbed energy to other molecules is thermalization.Thermalized energy carries no identity of the molecule that absorbed it.

Water vapor molecules can absorb (and emit) photonsat hundreds of wavelengths in the wavelength range of significant terrestrial thermal radiation(nearly all in the wavelength range 6-100 microns) compared to only one (15 micron) for CO_2 (wave length range of the single absorption band for $CO_2$is broadened to about 14-16 microns at sea level due to pressure, etc. but the multiple absorb/emit wave length bands for water vapor are equally broadened).

Reverse thermalization, where the warmed jostling molecules excite some molecules to emit a photon is almost entirely to water vapor molecules at sea level conditions. The reason is relaxation time of some water vapor moleculerotational emission lines is 0.5 µsec compared to 6µsec for CO_2 molecules and/or the thousands more 'opportunities' for emission by water vapor.

Water vapor has more 'opportunities' for emission because there are about 35 times as many water vapor molecules in the atmosphere below about 5 km as there are CO_2 molecules (See Figure 2) and each water vapor molecule has hundreds of emission bands compared to only one band for each CO_2 molecule. Most, if not all, of the photons emitted by the water vapor molecules are at wavelengths different from the narrow band CO_2 molecules can absorb. Effectively, energy absorbed by CO_2 is rerouted to space via water vapor.

At very high altitudes, molecule spacing and time between collision increases to where reverse-thermalization to CO_2 molecules becomes significant as does radiation from them to space.

Figure 1 is a typical graph showing top-of-atmosphere (TOA) thermal radiation from the planet. The TOA radiation from different locations on the planet can be decidedly different, e.g. as shown in Figure 9 of Reference [8]. Figure 1, here, might be over a temperate ocean and thus typical for much of earth's surface.
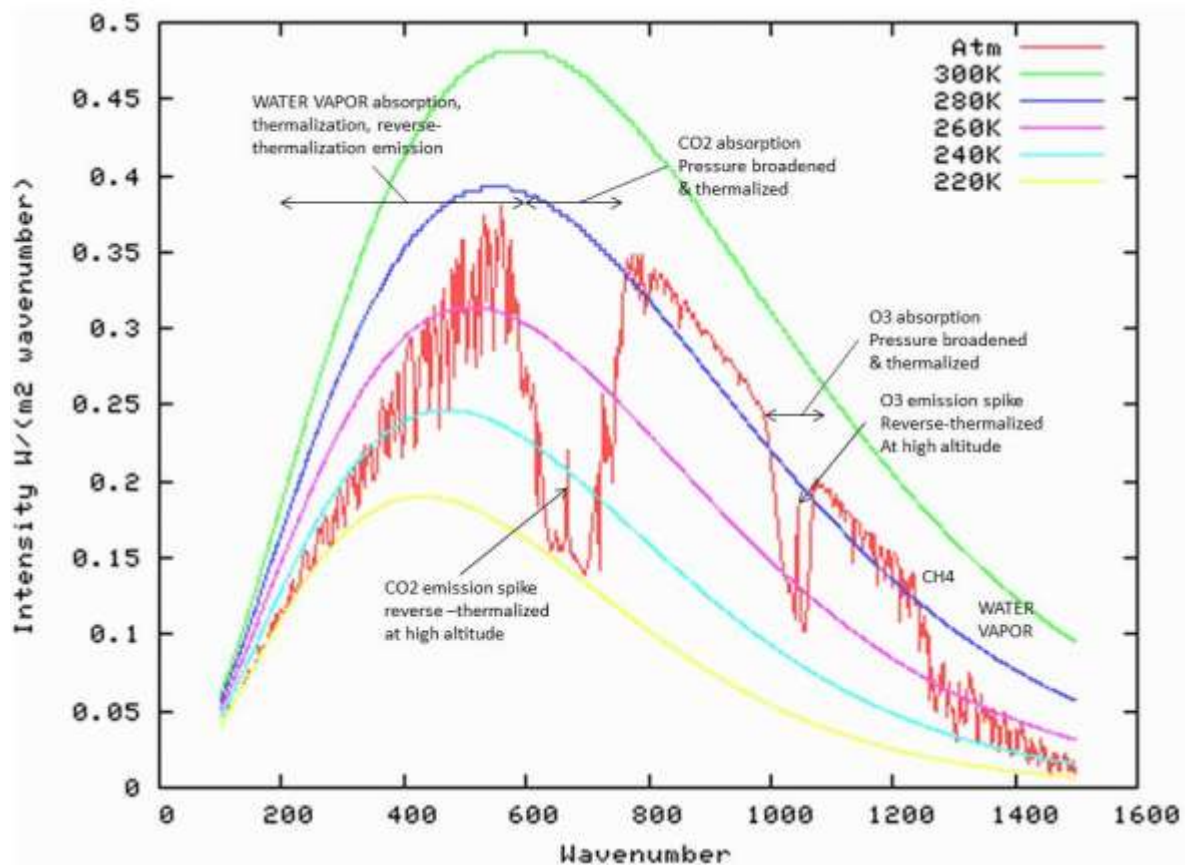

Figure 1: Terrestrial thermal radiation and absorption.

Approximately 98% of atmospheric molecules are non-ghg nitrogen and oxygen. They are substantially warmed by thermalization of the photonic energy absorbed by the ghg molecules.
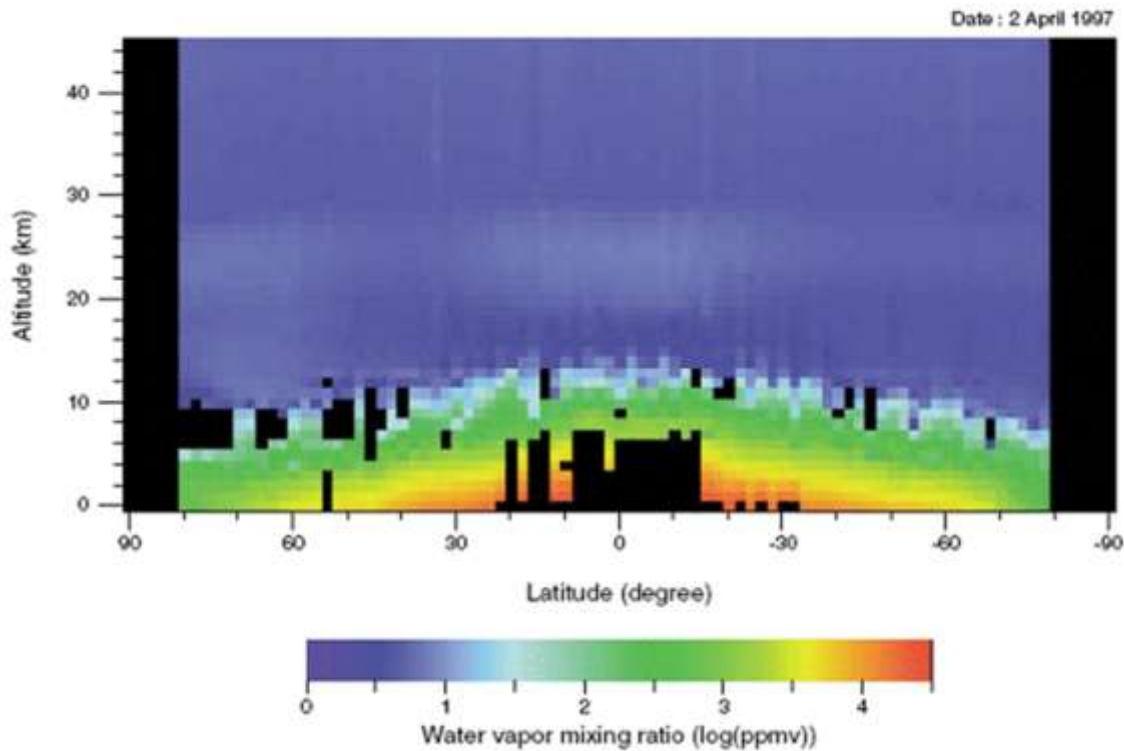

Figure 2: Water vapor declines rapidly with altitude.[9] (original from NASA)

Thermalized energy carries no identity of the molecule that absorbed it.The thermalized radiation warms the air, reducing its density, causing updrafts which are exploited by soaring birds, sailplanes, and occasionally hail. Updrafts are matched by downdrafts elsewhere, usually spread out but sometimes recognized by pilots and passengers as 'air pockets' and micro bursts.

A common observation of thermalization by way of water vapor is cloudless nights cool faster when absolute water vapor content of the atmosphere is lower.

Jostling between gas molecules (observed as temperature and pressure) sometimes causes reverse-thermalization. At low to medium altitudes, EMR emission stimulated by reverse-thermalization is essentially all by way of water vapor.

At altitudes below about 10 km a comparatively steep population gradient (decline with increasing altitude) in water vapor molecules favors outward radiation with increasing amounts escaping directly to space. At higher altitudes, increased molecule spacing and greatly diminished water vapor molecules favors reverse thermalization to CO_2. This is observed in the sharp peaks at nominal absorb/emit wavelengths of non-condensing ghg (See Figure 1).

Thermalization results in the influence of CO_2 on climate to be not significantly different from zero.

II. Environmental Protection Agency mistake
The US EPA asserts [10] Global Warming Potential (GWP) is a measure of "effects on the Earth's warming" with "Two key ways in which these [ghg] gases differ from each other are their ability to absorb energy (their "radiative efficiency"), and how long they stay in the atmosphere (also known as their "lifetime")."

The EPA calculation overlooks the very real phenomenon of thermalization. Trace ghg (all ghg except water vapor)have no significant effect on climate because absorbed energy is immediately thermalized.

Water vapor(Rev 8/26/16)
Water vapor is the ghg which makes earth warm enough for life as we know it. Increased atmospheric water vapor contributes to planet warming. Water vapor molecules are far more effective at absorbing terrestrial thermal radiation than CO_2 molecules (even if thermalization did not eliminate CO_2 as a significant warmer).Atmospheric water vapor has increased primarily ($\approx$ 98%) as a result of increased irrigation, with comparatively tiny contributions from cooling towers at electricity generating facilities, and increased burning of hydrogen rich fossil fuels especially natural gas which is nearly all methane. Of course increased water vapor causes the planet to warm which further increases water vapor so there is a cumulative effect (in control system analysis as done by engineers, this is called feedback. The term 'feedback' has a somewhat different meaning to Climate Scientists). This cumulative effect also amplifies cooldowns. More water vapor in the atmosphere means more warming,probably acceleration of the hydrologic cycleandincreased probability of floods.How much of recent flooding is simply bad luck in the randomness of weather and how much is because of the 'thumb on the scale' of added water vapor? Water vapor exhibits a logarithmic decline in effect of equal added increments (Fig. 3 of Ref. [12]).

Essentially all of the ghg effect on earth comes from water vapor. Clear air water vapor measurements over the non-ice-covered oceans in the form of total precipitable water (TPW) have been made since about 1987 by Remote Sensing Systems (RSS) [11].A graph of thismeasured 'global' averageanomaly data, with a reference value of 28.73 added,is shown in the left graph of Figure 3.The trend of this data is extrapolated both earlier and later using CO_2 level as a proxy, with the expression kg/m^2 TPW = 4.5118 * ppmvCO$_2$^0.31286. The result is the right-hand graph of Figure 3.(The 1940-1950 flat exists in the Law Dome CO_2 data base.)
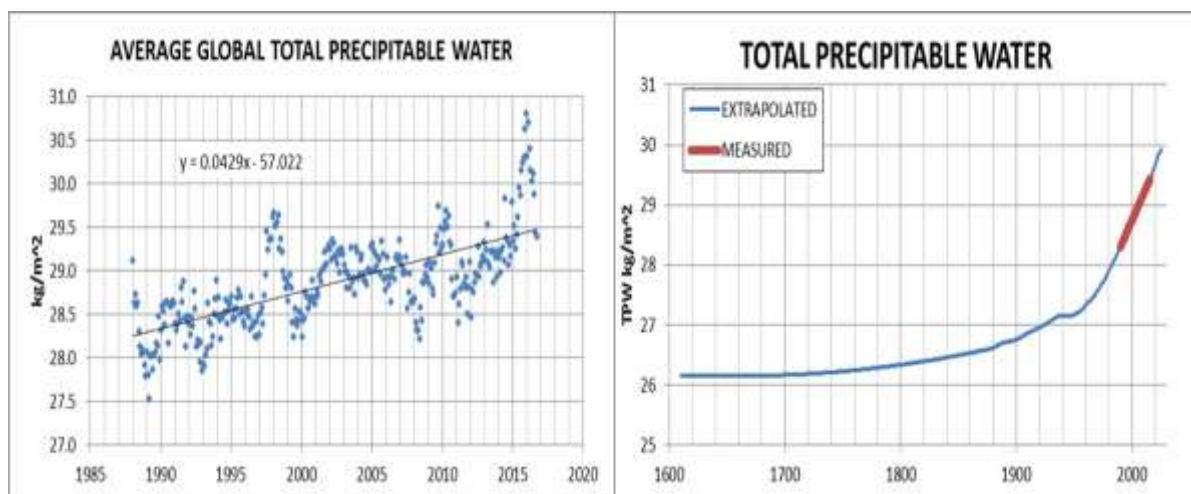

Figure 3: Average clear air total precipitable water over all non-ice-covered oceans.(Rev 8/26/16)

Clouds (average emissivity about 0.5) consist of solid and/or liquid water particles that radiate approximately according to Planck spectrum and Stephan-Boltzmann(S-B) law (each particle contains millions of molecules).

The perception water vapor content of the atmosphere depends even minutely on CO_2 content is profoundly misleading and precisely wrong because it ignores the partial pressure of water.

III.   The AGT Model

Most modeling of global climate has been with Global Climate Models (GCMs) where physical laws are applied to hundreds of thousands of discrete blocks and the interactions between the discrete blocks are analyzed using super computers with an end result being calculation of the AGT trajectory. This might be described as a 'bottom up' approach. Although theoretically promising, multiple issues currently exist with this approach.Reference [13]discloses that nearly all of the more than 100 current GCMs are obviously faulty. The few which appear to follow measurements might even be statistical outliers of the 'consensus' method. The growing separation between calculated and measured AGT as shown at Figure 17 in Ref. [14] alsosuggests some factor is missing.

The approach in the analysis presented here is 'top down'. This type of approach has been called 'emergent structures analysis'. As described by Dr. Roy Spencer in his book *THE GREAT GLOBAL WARMING*

BLUNDER, "Rather than model the system from the bottom up with many building blocks, one looks at how the system as a whole behaves." That approach is used here with strict compliance with physical laws.

The basis for assessment of AGT is the first law of thermodynamics, conservation of energy, applied to the entire planet as a single entity. Much of the available data are forcings or proxies for forcings which must be integrated (mathematically as in calculus, i.e. accumulated over time) to compute energy change. Energy change divided by effective thermal capacitance is temperature change. Temperature change is expressed as anomalies which are the differences between annual averages of measured temperatures and some baseline reference temperature; usually the average over a previous multiple-year time period. (Monthly anomalies, which are not used here, are referenced to previous average for the same month to account for seasonal norms.)

The AGT model, a summation of contributing factors, is expressed in this equation:

$$\text{Tanom} = (A,y) + \text{thcap}^{-1} * \Sigma^{y}_{i=1895} \{B*[S(i)-\text{Savg}] + C*\ln[\text{TPW}(i)/\text{TPW}(1895)] - F * [(T(i)/T(1895))^4 - 1]\} + D \quad\quad (1)$$

Where:
Tanom = Calculated average global temperature anomaly with respect to the baseline of the anomaly for the measured temperature data set, K
A = highest-to-lowestextent in the saw-tooth approximation of the net effect on planet AGT of all ocean cycles, K
y = year being calculated
(A,y) = value of the net effect of ocean cycles on AGT in year y (α-trend), K
thcap = effective thermal capacitance [1] of the planet = 17 ± 7 W yr m^{-2} K^{-1}
1895 = Selected beginning year of acceptably accurate world wide temperature measurements.
B = combined proxy factor and influence coefficient for energy change due to sunspot number anomaly change, Wyr m^{-2}
S(i) = average daily V2 sunspot numbers [15,16] in year i
Savg = baseline for determining SSN anomalies
C = influence coefficient for energy change due to TPWchange, Wyr m^{-2}
TPW(i) = total precipitable water in year i, kg m^{-2}
TPW(1895) = TPW in 1895, same units as TPW(i)
F = 1 to account for change to S-B radiation from earth due to AGT change, W yr m^{-2}
T(i) = AGT calculated by adding T(1895) to the reported anomaly, K
T(1895) = AGT in 1895 = 286.707 K
D = offset that shifts the calculated trajectory vertically on the graph, without changing its shape, to best match the measured data, K (equivalent to changing the anomaly reference temperature).

Accuracy of the model is determined using the Coefficient of Determination, R^2, to compare calculated AGT with measured AGT.

Approximate effect on the planet of the net of ocean surface temperature (SST)
The average globalocean surface temperature oscillation is only about $\pm1/6$ K. Itis defined to *not significantly add or remove planet energy*. The net influence of SST oscillation on reported AGT is defined as α-trend. In the decades immediately prior to 1941 the amplitude range of the trends was not significantly influenced by change to any candidate internal forcing effect; so the observed amplitude of the effect on AGT of the net ocean surface temperature trend anomaly then, must be approximately the same as the amplitude of the part of the AGT trend anomaly due to ocean oscillations since then. This part is approximately 0.36 K total highest-to-lowest extent with a period of approximately 64 years (verified by high R^2 in Table 1).

The measured AGT trajectory (Figure 9) suggests that the least-biased simple wave form of the effective ocean surface temperature oscillation is approximately saw-toothed. Approximation of the sea surface temperature anomaly oscillation can be described as varying linearly from $-A/2$ K in 1909 to approximately $+A/2$ K in 1941 and linearly back to the 1909 value in 1973. This cycle repeats before and after with a period of 64 years.

Because the actual magnitude of the effect of ocean oscillation in any year is needed, the expression to account for the contribution of the ocean oscillation in each year to AGT is given by the following:

$$\Delta Tosc = (A,y) \qquad K \text{ (degrees)} \qquad (2)$$

where the contribution of the net of ocean oscillations to AGT change is the magnitude of the effect on AGT of the surface temperature anomaly trend of the oscillation in year y, and **A** is the maximum highest-to-lowest extent of the effect on AGT of the net ocean surface temperature oscillation.
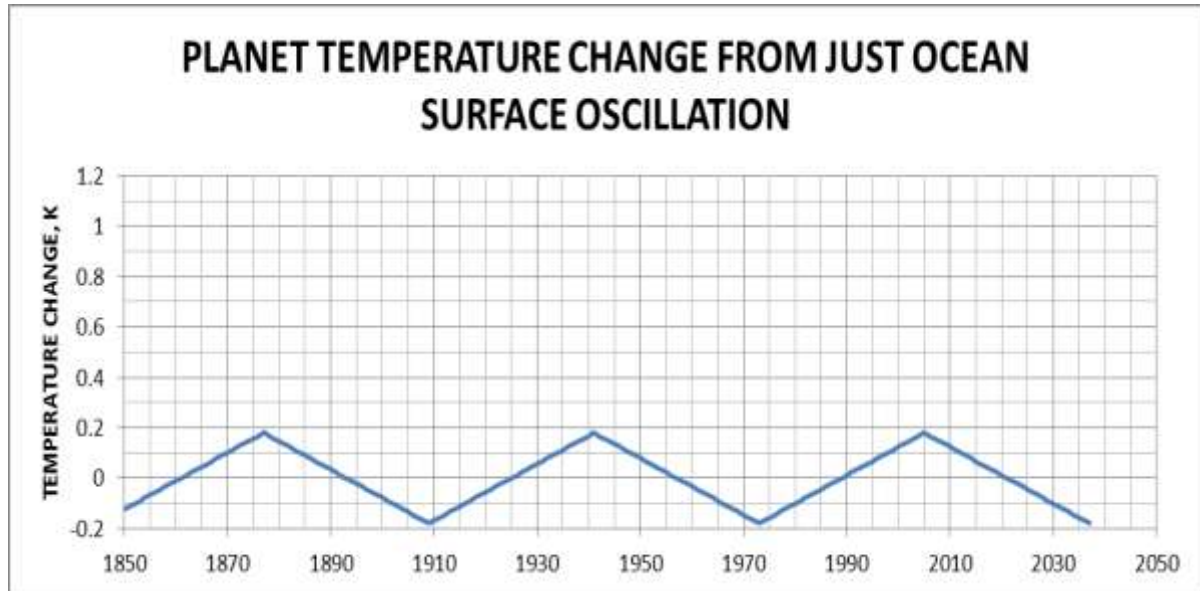
Equation (2) is graphed in Figure 4 for A=0.36.

Figure 4: Ocean surface temperature oscillations (α-trend) do not significantly affect the bulk energy of the planet.

Comparison of approximation with 'named' ocean cycles

Named ocean cycles include, in the Pacific north of 20N, Pacific Decadal Oscillation (PDO); in the equatorial Pacific,El Nino Southern Oscillation (ENSO); and in the north Atlantic, Atlantic Multidecadal Oscillation (AMO).

Ocean cycles are perceived to contribute to AGT in two ways: The first is the direct measurement of sea surface temperature (SST). The second is warmer SST increases atmospheric water vapor which acts as a forcing and therefore has a time-integral effect on temperature. The approximation, (A,y), accounts for both ways.

SST data is available for three named cycles: PDO index, ENSO 3.4 index and AMO index. Successful accounting for oscillations is achieved for PDO and ENSO when considering these as forcings (with appropriate proxy factors) instead of direct measurements. As forcings, their influence accumulates with time. The proxy factors must be determined separately for each forcing. The measurements are available since 1900 for PDO [17] and ENSO3.4 [18]. This PDO data set has the PDO temperature measurements reduced by the average SST measurements for the planet.

The contribution of PDO and ENSO3.4 to AGT is calculated by:
$$PDO\_NINO = \Sigma^{y}_{i=1900} (0.017*PDO(i) + 0.009 * ENSO34(i)) \qquad (3)$$

Where:

PDO(i) = PDO index [17] in year i
ENSO34(i) = ENSO 3.4 index [18] in year i

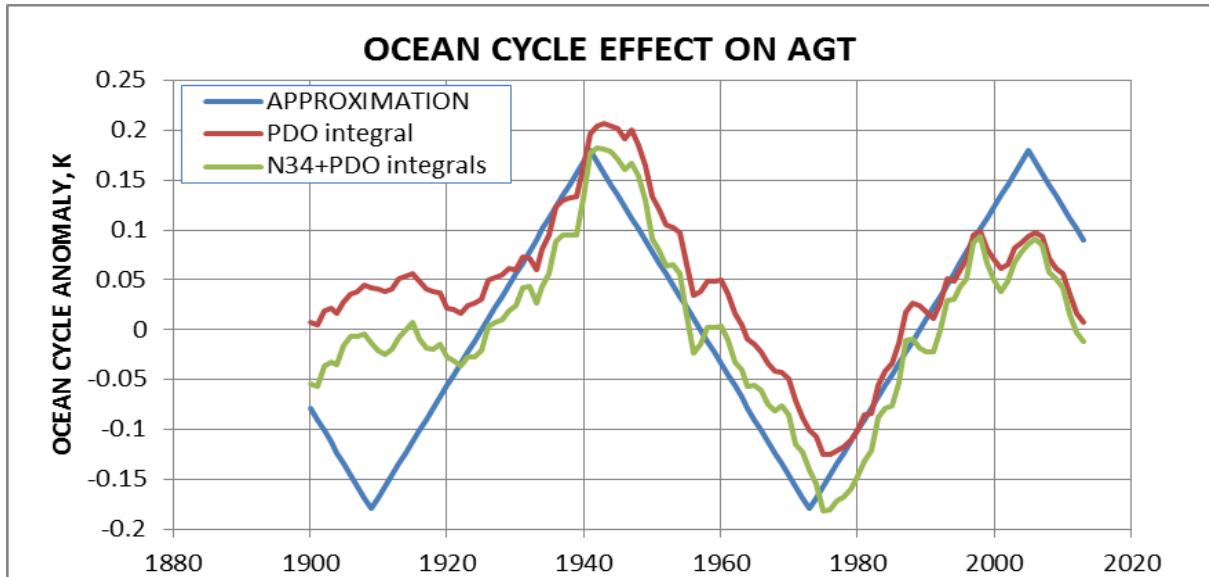How this calculation compares to the idealized approximation used in Equation (2) with A = 0.36 is shown in Figure 5.

Figure 5: Comparison of idealized approximation of ocean cycle effect and the calculated effect from PDO and ENSO.

The AMO index [19] is formed from area-weighted and de-trended SST data. It is shown with two different amounts of smoothing in Figure 6 along with the saw-tooth approximation for the entire planet per Equation (2) with A = 0.36.
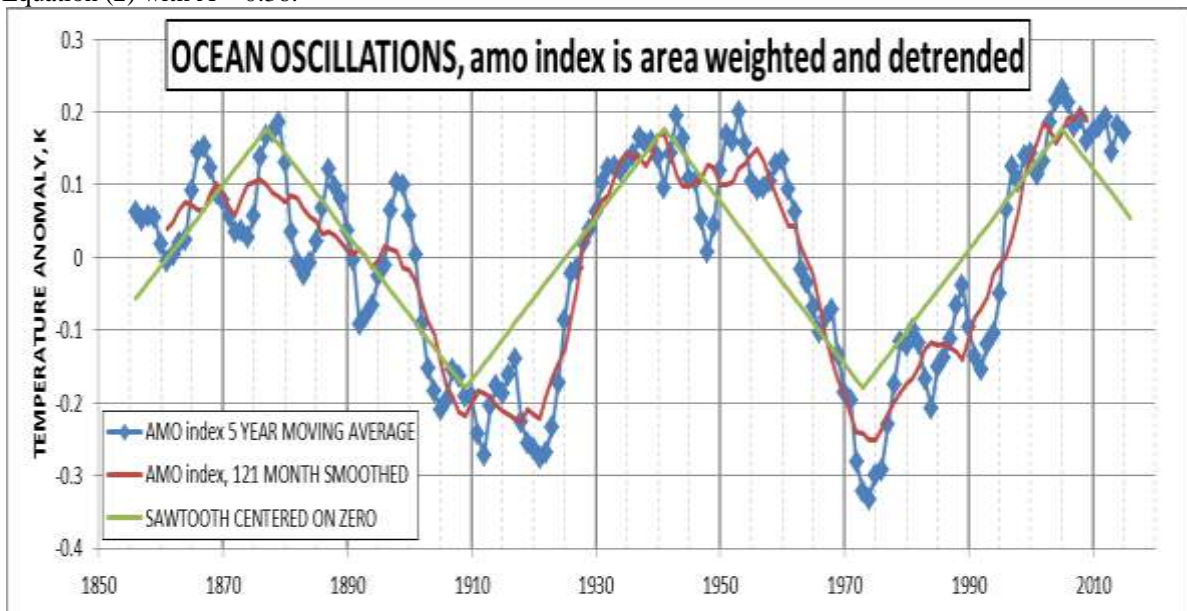

Figure 6: Comparison of idealized approximation of ocean cycle effect and the AMO index.

The high Coefficients of Determination in Table 1 and the comparisons in Figures 5 and 6 corroborate the assumption that the saw-tooth profile with a period of 64 years provides adequate approximation of the net effect of all named and unnamed ocean cycles in the calculated AGT anomalies.

IV.   ATMOSPHERIC CARBON DIOXIDE

The level of atmospheric carbon dioxide (CO_2) has been widely measured over the years. Values from ancient times were determined by measurements on gas bubbles which had been trapped in ice cores extracted from Antarctic glaciers [20]. Spatial variations between sources have been found to be inconsequential [2]. The best current source for atmospheric carbon dioxide level [21] is Mauna Loa, Hawaii. Extrapolation to future CO_2 levels, shown in Figure 7, is accomplished using a second-order curve fit to data measured at Mauna Loa from 1980 to 2012.
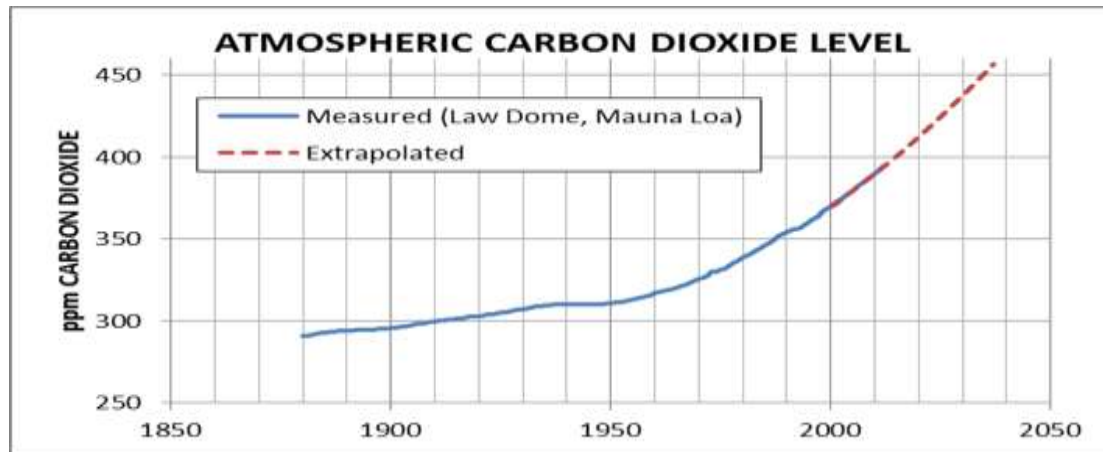
Figure 7: Measured atmospheric carbon dioxide level since 1880 and extrapolation to 2037.

Sunspot numbers

Sunspots have been regularly recorded since 1610.In 2015 historical (V1) SSN were reevaluated in light of current perceptions and more sensitive instruments and are designated as V2. The V2 SSN data set is used throughout this assessment.V2 SSN [15]are shown in Figure 8.

Sunspot numbers (SSN) are seen to be in cycles each lasting approximately 11 years. The current cycle, called 24, has been comparatively low, has peaked, and isnow in decline.

The Maunder Minimum (1645-1700), an era of extremely low SSN, was associated with the Little Ice Age. The Dalton Minimum (1790-1820) was a period of low SSN and low temperatures. An unnamed period of low SSN (1880-1930) was also accompanied by comparatively low temperatures.

An assessment of this is that sunspots are somehow related to the net energy retained by the planet, as indicated by changes to the average global temperature trend. Fewer sunspots are associated with cooling, and more sunspots are associated with warming. Thus the hypothesis is made that SSN are proxies for the rate at which the planet accumulates (or loses) radiant energy over time. Thereforethe time-integral of the SSN anomaliesis a proxy for most of the amount of energy retained by the planet above or below breakeven.

Also, a lower solar cycle over a longer period might result in the same increase in energy retained by the planet as a higher solar cycle over a shorter period. Both magnitude and time are accounted for by taking the time-integral of the SSN anomalies, which is simply the sum of annual mean SSN (each minus Savg) over the period of study.

SSN change correlates with change to Total Solar Irradiance (TSI). However, TSI change can only account for less than 10% of the AGT change on earth. Because AGT change has been found to correlate with SSN change, the SSN change must act as a catalyst on some other factor (perhaps clouds [22]) which have a substantial effect on AGT.
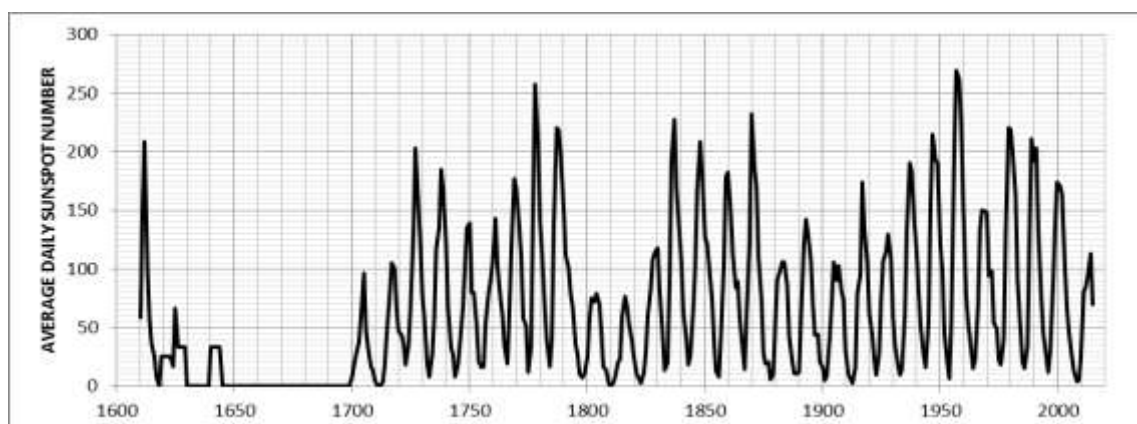

Figure 8:V2 SSN [15]

Possible values for Savg are subject to two constraints. Initially they are determined as that which results in derived coefficients and maximum R^2. However, calculated values must also result in rational values for calculated AGT at the depths of the Little Ice Age. The necessity to calculate a rational LIA AGT is a somewhat more sensitive constraint. The selected value for Savg results in calculated LIA AGT of approximately 1 K less than the recent trend which appears rational and is consistent with most LIA AGT assessments.

AGT measurement data set
In the last few years, reported temperature data, especially land temperature data, have been changed by the reporting agencies. This detracts from their applicability in any correlation.

Rapid year-to-year changes in reported temperature anomalies are not physically possible for true energy change of the planet. The sharp peak in 2015, which coincides with an extreme El Nino, is especially distorting. It, at least in part, will be compensated for by a La Nina which is likely to follow. For analysis here, the El Nino spike is compensated for by replacing reported AGT for 2013-2015 with the average 2002-2012.

A further bit of confusion is introduced by satellite determinations. Anomalies they report as AGT anomalies are actually for the lower troposphere (LT), have a different reference temperature (reported anomalies determined using satellite data are about 0.2 K lower), and appear to be somewhat more volatile (about 0.15 K further extremes than surface measurements) to changes in forcing.

The data set used for this assessment is the current (5/27/16)HadCRUT4 data set [23] through 2012 with 2013-2015 set at the average 2002-2012 at 0.4863 K above the reference temperature. This set is shown in Figure 9.
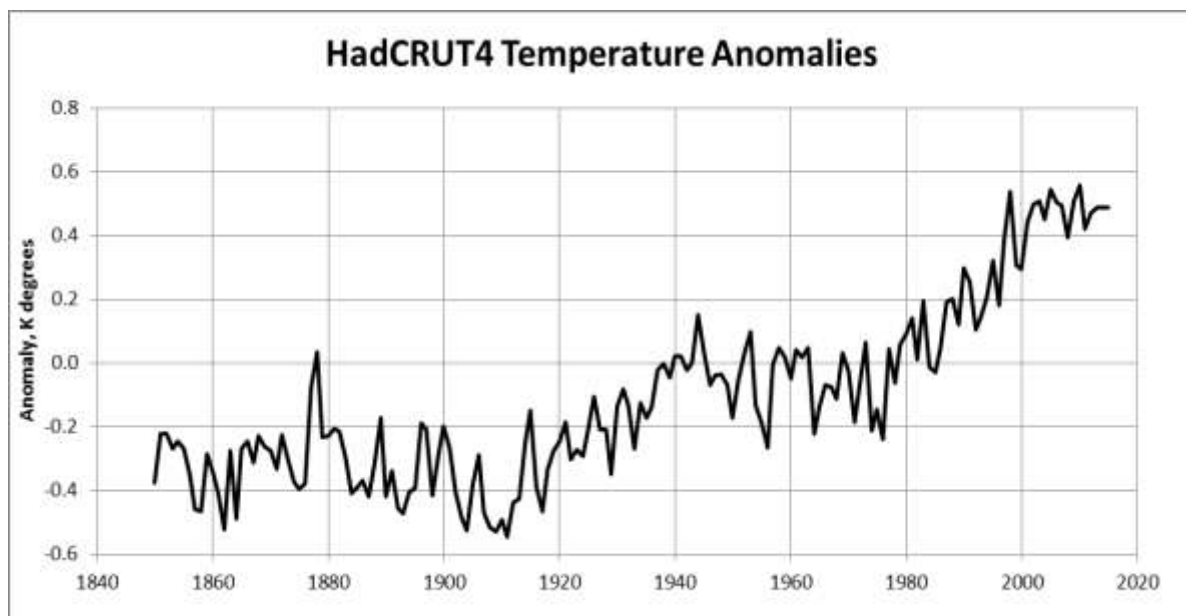

Figure 9: HadCRUT4 data set as of 5/27/16 with flat starting in 2013 as used here.

The sunspot number anomaly time-integral is a proxy for a primary driver of the temperature anomaly β-trend
By definition, energy change divided by effective thermal capacitance is temperature change.

In all cases in this document, coefficients (A, B, C, D& F) which achieved maximum R^2 for unsmoothed data sets were not changed when calculating R^2 for smoothed data.

Incremental convergence to maximum R^2 is accomplished by sequentially and repeatedly adjusting the coefficients. The process is analogous to tediously feeling the way along a very long and narrow mathematical tunnel in 4-dimensional mathematical space. The 'mathematical tunnel' is long and narrow because the influence on AGT determined by the SSN anomaly time-integral, at least until the last decade or so, is quite similar to the influence on AGT as determined by the rise in TPW.

Measured temperature anomalies in Figure 10areHadCRUT4 data as shown in Figure 9. The excellent match of the up and down trends since before 1900 of calculated and measured temperature anomalies, shown here in Figure 10, and, for 5-year moving average smoothed temperature anomaly measurements, in Figure 11,demonstrate the usefulness and validity of the calculations. All reported values since before 1900 are within the range ±2.5 sigma (±0.225 K) from the calculated trend.Note: The variation is not in the method, or the measuring instruments themselves, but results from the effectively roiling (at this tiny magnitude of temperature change) of the object of the measurements.

Projection until 2020 uses the expected sunspot number trend for the remainder of solar cycle 24 as provided [16] by NASA. After 2020 the 'limiting cases' are either assuming sunspots like from 1924 to 1940 or for the case of no sunspots which is similar to the Maunder Minimum.

Some noteworthy volcanoes and the year they occurred are also shown on Figure 10. No consistent AGT response is observed to be associated with these. Any global temperature perturbation that might have been caused by volcanoes of this size is lost in the natural fluctuation of measured temperatures.

Much larger volcanoes can cause significant temporary global cooling from the added reflectivity of aerosols and airborne particulates. The Tambora eruption, which started on April 10, 1815 and continued to erupt for at least 6 months, was approximately ten times the magnitude of the next largest in recorded history and led to 1816 which has been referred to as 'the year without a summer'. The cooling effect of that volcano exacerbated the already cool temperatures associated with the Dalton Minimum.
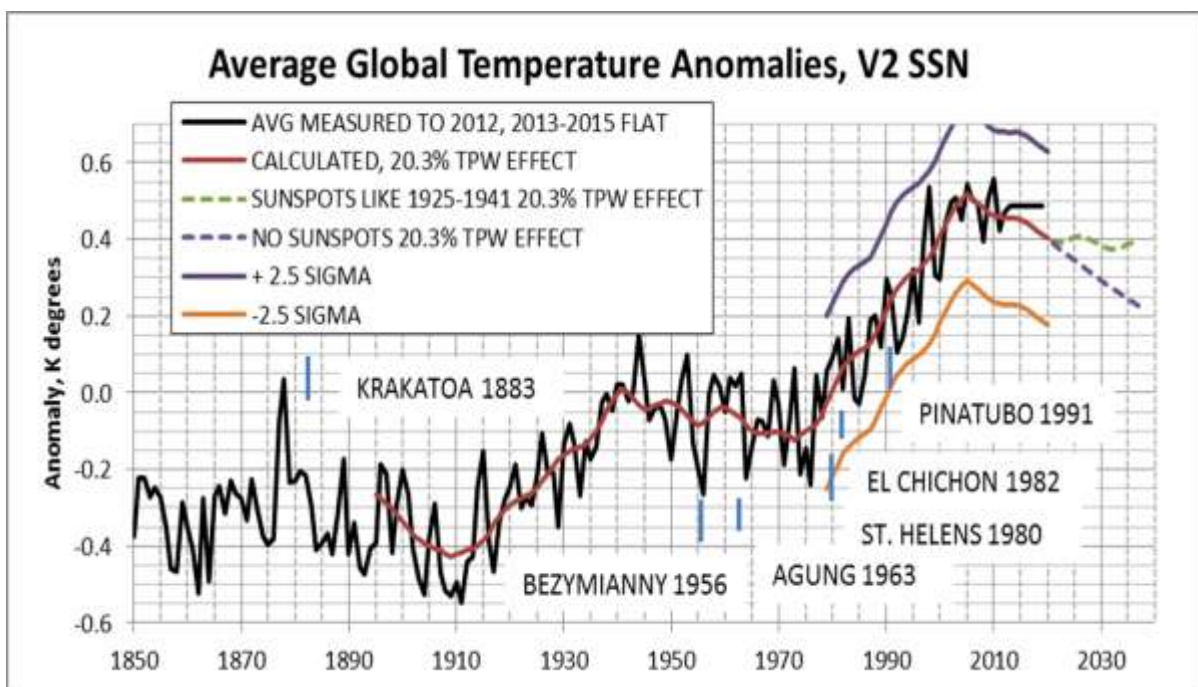

Figure 10: Measured average global temperature anomalies with calculated future trendsusing Savg = 60and with V2 SSN. R ^{2} = 0.904520.(Rev 8/26/16)

Coefficients in Equation (1) which were determined by maximizing R^2 identify maximums for each of the factors explicitly considered. Factors not explicitly considered (such as unaccounted for residual (apparently random)variation in reported annual measured temperature anomalies, aerosols, CO_2, other non-condensing ghg, volcanoes, ice change, etc.) must find room in the unexplained residual, and/or by occupying a fraction of the effect otherwise occupied by each of the factors explicitly considered.
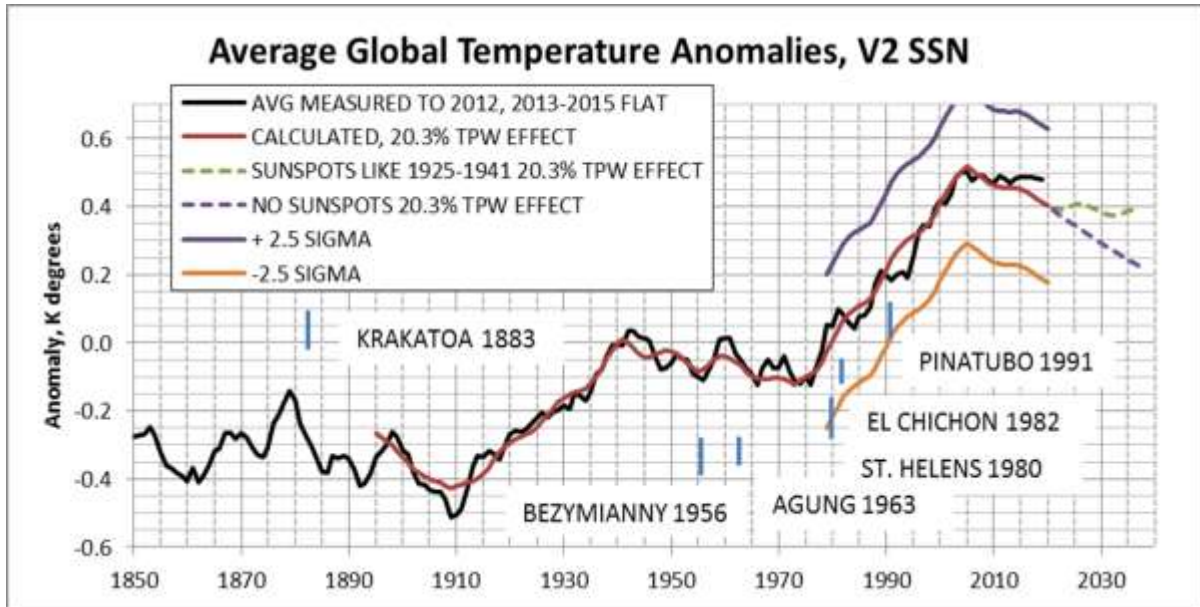
Figure 11: Same as Figure 10 but with 5-year running average of measured temperatures. R^2 = 0.981782.(Rev 8/26/16)

The derived coefficients and other results are summarized in Table 1. Note that a coefficient of determination, R^2 = 0.981782 means a near-perfect correlation coefficient of 0.99.

The influence of the net effect of factors other than the net effect of ocean cycles on AGT can be calculated by excluding the α-trend (set 'A' to zero) from the AGT which was calculated using Equation (1). For the values used in Figure 10, thisresults in the β-trend as shown in Figure 12. Note that in 2005 the anomaly from other than α-trend, as shown in Figure 12, is A/2 lower than the calculated trend in Figures 10 and 11 as it should be.

Figure 12: Anomaly trend (β-trend).Equation (1) except summation starts at i = 1610 and excluding α-trend. (Rev 8/26/16)

How the β-trend could take place

Although the connection between AGT and the sunspot number anomaly time-integral is demonstrated, the mechanism by which this takes place remains somewhat speculative.

Various papers have been written that indicate how the solar magnetic field associated with sunspots can influence climate on earth. These papers posit that decreased sunspots are associated with decreased solar magnetic field which decreases the deflection of and therefore increases the flow of galactic cosmic rays on earth.

Henrik Svensmark, a Danish physicist, found that increased flow of galactic cosmic rays on earth caused increased low altitude (<3 km) clouds and planet cooling. An abstract of his 2000 paper is at [24]. Marsden and Lingenfelter also report this in the summary of their 2003 paper [25] where they make the statement "…solar activity increases…providing more shielding…less low-level cloud cover…increase surface air temperature." These findings have been further corroborated by the cloud nucleation experiments [26] at CERN.

These papers [24,25] associated the increased low-altitude clouds with increased albedo leading to lower temperatures. Increased low altitude clouds would also result in lower average cloud altitude and therefore higher average cloud temperature. Although clouds are commonly acknowledged to increase albedo, they also radiate energy to space so increasing their temperature increases S-B radiation to space which would cause the planet to cool. Increased albedo reduces the energy received by the planet and increased radiation to space reduces the energy of the planet. Thus the two effects work together to change the AGT of the planet.

A contributing or possibly alternate speculation is that clouds might also be affected by solar wind. End result is the same: Average global temperature correlates with the time-integral of sunspot number anomalies (when combine with two other factors as shown in Equation (1)).

Simple analyses [22] indicate that either an increase of approximately 186 meters in average cloud altitude or a decrease of average albedo from 0.3 to the very slightly reduced value of 0.2928 would account for all of the 20th century increase in AGT of 0.74 K. Because the cloud effects work together and part of the temperature change is due to ocean oscillation (low in 1901, 0.2114 higher in 2000), substantially less cloud change would suffice.

Hind Cast Estimate

Average global temperatures were not directly measured in 1610 (accurate thermometers had not been invented yet). Recent estimates, using proxies, are few. The temperature anomaly trend that Equation (1) calculates for that time is roughly consistent with other estimates. The decline in the trace 1615-1715 on Figure 12 results from the low sunspot numbers for that period as shown on Figure 8.

As a possibility, the period and amplitude of oscillations attributed to ocean cycles demonstrated to be valid after 1895 are assumed to maintain back to 1610.Equation (1)is modified to begin integration in 1610. The coefficient D is changed to make the calculated temperature in 2005 equal to what it is in Figure 10.

Temperature anomalies thus calculated, estimate possible trends since 1610 and actual trends of reported temperatures since they have been accurately measured worldwide. This assessment is shown in Figure 13.
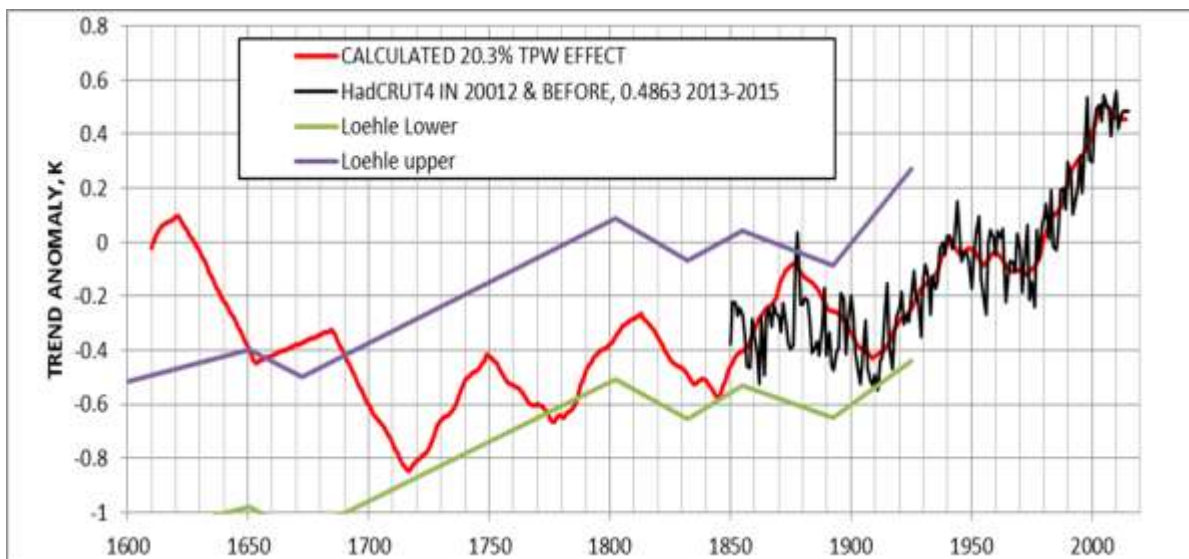

Figure 13: Calculated temperature anomalies using Equation (1) withthe same coefficients as for Figure 10 and V2 SSN.Measured temperature anomalies from Figure 9, and anomaly range estimates determined by Loehle are superimposed.(Rev 8/26/16)

A survey [27] of non-tree-ring global temperature estimates was conducted by Loehle including some for a period after 1610. Simplifications of the 95% limits found by Loehle are also shown on Figure 13. The spread between the upper and lower 95% limits are fixed, but, since the anomaly reference temperatures might be different, the limits are adjusted vertically to approximately bracket the values calculated using Equation (1). The fit appears reasonable considering the uncertainty of all values.

Calculated temperature anomalies look reasonable back to 1700 but indicate higher temperatures prior to that than most proxy estimates. They are, however, consistent with the low sunspot numbers in that period. They qualitatively agree with Vostok, Antarctica ice core data but decidedly differ from SargassoSea estimates during that time (see the graph for the last 1000 years in Reference [2]). Worldwideassessments of average global temperature, that far back,are sparse and speculative. Ocean oscillations might also have been different from assumed.

Projection from 1990
Figure 14 shows the calculation using Equation (1) with coefficients determined using HadCRUT4 measured temperatures to 1990. The calculated AGT trend in 2020 projected from 1990is 0.06 K cooler than the projection from 2015.
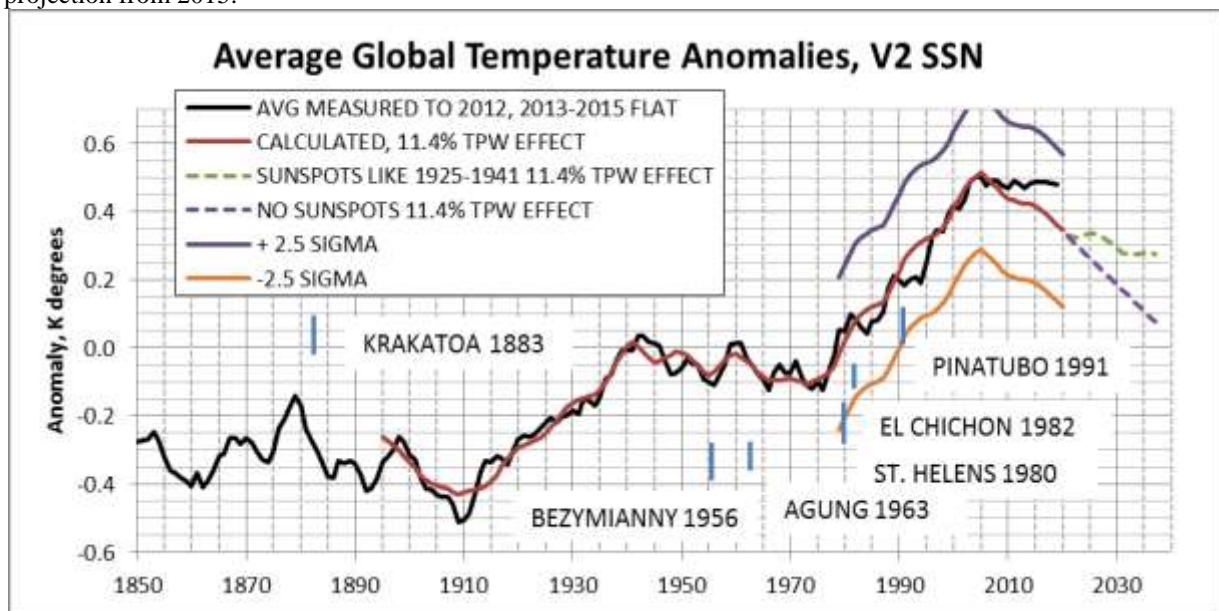

Figure 14: Same as Figure 11 except coefficients determined using data through 1990.

Step changes in AGT
Interpretation of a reported sudden AGT increase (or decrease) as planet energy increase (or decrease) is physically impossible because of the huge effective thermal capacitance which results in a 5-year time constant [1] for thermal response of the planet to a step change in forcing.

Influence of atmosphericwater vapor on AGT
The temperature increase through 2015 attributable to TPW is the net of the increase from TPW and the decrease from added S-B radiation due to the part of the temperature riseattributable to TPW which is above the 1895 value of 286.707 K. The net effect is designated ΔT_{TPW}.

At least until the last decade or so, the influence on AGT due to TPW has been quite similar to the influence on AGT determined by the SSN anomaly time-integral. This similarity has resulted in the effect of TPWbeing erroneously masked by the calculated effect of sunspot number anomalies.

Figure 15 shows how increasing water vapor has contributed to AGT. It is the same as Figure 11 but shows also the calculated trajectory if there had been no increase in water vapor since 1895. This is calculated by setting C to zero and retaining the other coefficients in Equation (1).

The temperature increase from water vapor increase is, on average, somewhat less than the water vapor increase from temperature increase but still results in a substantial feedback effect. The feedback effect results in

amplification of a small increase in water vapor from other cause (wind or ??). It is speculated that local conditions might result in a local thermal runaway which is observed as a super el Niño. The sharp spike and following la Nina are consistent with this hypothesis.
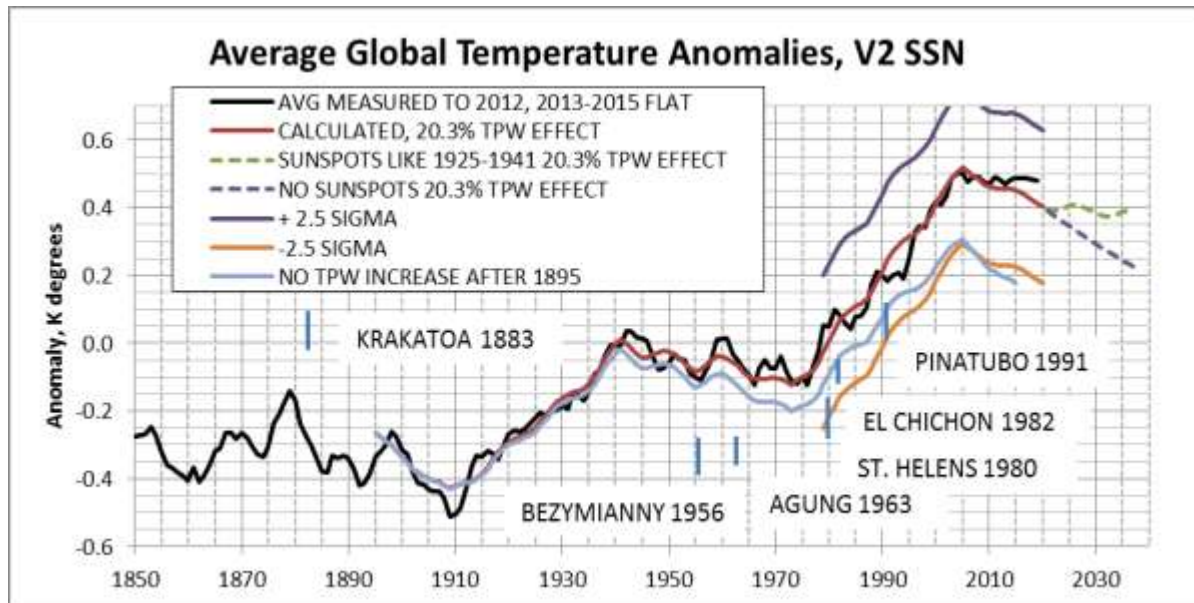

Figure 15: Same as Figure 11 but with trajectory incorporated for the case if there was no increase in water vapor since 1895.(added 10/31/16)

Values for the coefficients and results are summarized in Table 1.

Table 1: A, B, C, D, F refer to coefficients in Equation 1. The column headed # is a code identifying the particular EXCEL file used.(Rev 8/26/16)

#	Fig	Savg	OCEAN A	SUN B	TPW C	Δ D	F	R^2	5-YR R^2	1895-2015 ΔT_{TPW}K	% CAUSE OF 1909-2005 AGT CHANGE		
											Sun	SEA	TPW
E	10	60	.36	.00205	1.24	-.428	1	.904520	.981782	.261	38.0	41.7	20.3
C	14	60	.370	.00244	.557	-.430	1	.78067	.957356	.152	49.5	39.1	11.4
G	15	60	.36	.00205	0	-.428	1	.76	.83	0	52.1	47.9	0

V.   CONCLUSIONS

Three factors explain essentially all of AGT change since before 1900. They are ocean cycles, accounted for with an approximation, influence quantified by a proxy; the SSN anomaly time-integraland, the gain in atmospheric water vapor measured since 1987 and extrapolated before and after using measured CO_2 as a proxy.

Othershave looked at only amplitude or only duration factors for solar cycles and gotpoor correlations with average global temperature. The excellent correlation comes by combining the two, which is what the time-integral of sunspot number anomalies does. Prediction of future sunspot numbers more than a decade or so into the future has not yet been confidently done.

As displayed in Figure 12, the β-trend shows the estimated true average global temperature trend (the net average global energy trend)during the planet warm up from the depths of the Little Ice Age.

The net effect of ocean oscillations is to cause the surface temperatureα-trend to oscillate above and below theβ-trend. Equation (1) accounts for both trends.

Figure 11shows the near perfect match with calculated temperatures which occurs when random fluctuation in reported measured temperatures is smoothed out with 5-year moving average.

Warming attributed to increasing water vapor explains the flat measured AGT trend in spite of declining sunspot and ocean cycle forcings and might delay or even prevent global cooling.

Transitioning from coal to hydrogen rich fossil fuels might lead to increased flooding.

Long term prediction of average global temperatures depends primarily on long term prediction of sunspot numbers.

REFERENCES: (rev 10/21/16)

[1]. Effective thermal capacitance & time constant: Schwartz, Stephen E., (2007) Heat capacity, time constant, and sensitivity of earth's climate system, *J. Geophys. Res., vol. 113, Issue D15102*, doi:10.1029/2007JD009373

[2]. On line at http://www.ecd.bnl.gov/steve/pubs/HeatCapacity.pdf

[3]. 2008 assessment of non-condensing ghg http://www.middlebury.net/op-ed/pangburn.html

[4]. Phanerozoic AGT & CO_2: http://www.geocraft.com/WVFossils/Carboniferous_climate.html

[5]. Phanerozoic AGT & CO_2: http://mysite.science.uottawa.ca/idclark/courses/Veizer%20Nature%202001.pdf

[6]. 5. 6 microsecond relaxation time in atmosphere http://onlinelibrary.wiley.com/doi/10.1002/qj.49709540302/abstract   10 microsecond CO2 relaxation in atmosphere: https://www.reddit.com/r/climateskeptics/comments/14hvl9/ucar_presents_a_cartoon_to_misrepresent_what/https://lofi.physforum.com/Greenhouse-Gas-Effect-and-Carbon-Dioxide_7157.html

[7]. 7.1 microsecond CO2 relaxation in pure gas http://pubs.rsc.org/en/Content/ArticleLanding/1967/TF/TF9676302093#!divAbstract).

[8]. Time between molecule collisions: http://hyperphysics.phy-astr.gsu.edu/hbase/kinetic/frecol.html

[9]. Barrett TOA radiationhttp://www.warwickhughes.com/papers/barrett_ee05.pdf

[10]. Water vapor vs altitude http://homeclimateanalysis.blogspot.com/2010/01/earth-radiator.html

[11]. EPA GWPhttps://www3.epa.gov/climatechange/ghgemissions/gwps.html

[12]. NASA/RSS TPWhttp://www.remss.com/measurements/atmospheric-water-vapor/tpw-1-deg-product

[13]. ftp://ftp.remss.com/vapor/

[14]. ftp://ftp.remss.com/vapor/monthly_1deg/

[15]. The above sequence of 3 links leads to this one with last digits of last number being the latest month

[16]. ftp://ftp.remss.com/vapor/monthly_1deg/tpw_v07r01_198801_201609.time_series.txt

[17]. Willis TPW graph: https://wattsupwiththat.com/2016/07/25/precipitable-water

[18]. Epic fail of 'consensus' method http://www.drroyspencer.com/2013/06/still-epic-fail-73-climate-models-vs-measurements-running-5-year-means

[19]. Analysis sans water vapor: http://globalclimatedrivers.blogspot.com

[20]. V2 sunspot numbers http://www.sidc.be/silso/datafiles

[21]. Graphic of V2 Solar cycle 24: http://solarscience.msfc.nasa.gov/predict.shtml

[22]. PDO index http://jisao.washington.edu/pdo/PDO.latest

[23]. El Nino 3.4 index http://www.esrl.noaa.gov/psd/gcos_wgsp/Timeseries/Data/nino34.long.data (Linked from http://www.cgd.ucar.edu/cas/catalog/climind/TNI_N34)

[24]. AMO index http://www.esrl.noaa.gov/psd/data/correlation/amon.us.long.data

[25]. CO2 level at Law Dome, Antarctica: http://cdiac.ornl.gov/ftp/trends/co2/lawdome.combined.dat

[26]. Mauna Loa CO2: ftp://aftp.cmdl.noaa.gov/products/trends/co2/co2_annmean_mlo.txt

[27]. Sensitivity of AGT to clouds http://lowaltitudeclouds.blogspot.com

[28]. Current HadCRUT4 data set: http://www.metoffice.gov.uk/hadobs/hadcrut4/data/current/time_series/HadCRUT.4.4.0.0.annual_ns_avg.txt

[29]. Svensmark paper: *Phys. Rev. Lett*. 85, 5004–5007 (2000)http://prl.aps.org/abstract/PRL/v85/i23/p5004_1

[30]. Marsden &Lingenfelter 2003, *Journal of the Atmospheric Sciences* 60: 626-636http://www.co2science.org/articles/V6/N16/C1.php

[31]. CLOUD experiment at CERN http://indico.cern.ch/event/197799/session/9/contribution/42/material/slides/0.pdf

[32]. Loehle non-tree-ring AGT http://www.econ.ohio-state.edu/jhm/AGW/Loehle/Loehle_McC_E&E_2008.pdf